CRYSTAL GROWTH & DESIGN

pubs.acs.org/crystal

Article

Utilizing Ionic Liquids as Bifunctional Reagents for the Ionothermal Synthesis of Uranyl Compounds

Daniel E. Felton, Tsuyoshi A. Kohlgruber, Zachary D. Tucker, Eva M. Gulotty, Brandon L. Ashfeld,* and Peter C. Burns*

Cite This: *Cryst. Growth Des.* 2023, 23, 8311−8318

Read Online

ACCESS | Metrics & More | Article Recommendations | Supporting Information

ABSTRACT: The extraction of actinides, specifically uranyl and other actinyl ions, from fission products is a critical aspect of spent nuclear fuel reprocessing. In this study, ionothermal syntheses were conducted to control the formation of uranyl $(UO_2)^{2+}$ salt complexes generated by exposure to a selection of ionic liquids (ILs). The high-thermal stability and ligation potential of ILs were exploited in a multifaceted approach toward uranyl salt complexation by enabling ligation of the IL anionic component while simultaneously providing polar reaction media to promote speciation. Furthermore, an evaluation of uranyl complex templating by the IL cation revealed that small, heterocyclic cationic molecules resulted in more densely packed anionic clusters. The uranium source was also varied to determine the oxidizing effect of nitrate on the ILs and the propensity for nitrate and acetate byproduct formation. Uranyl triflate was found to be the optimal uranium source for the production of pure uranyl complexes. The degree to which nitrate oxidizes the ILs was investigated to determine what oxidation products form and subsequently coordinate to the uranyl ion. Finally, it was shown that a uranyl succinate framework can be synthesized in high yield from an IL that contains succinate as the anion.

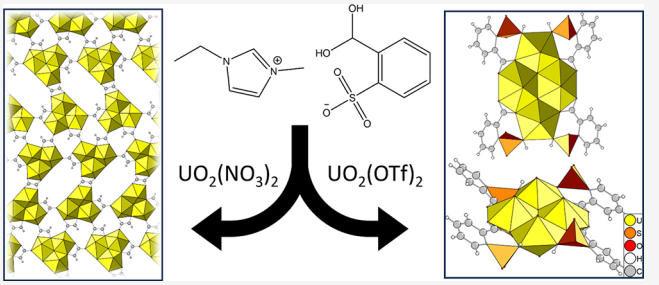

INTRODUCTION

The structural chemistry of uranium has expanded greatly over the last two decades as advances in X-ray diffraction techniques have allowed faster and more robust determination of crystal structures.[1] Compounds synthesized under aqueous conditions are dominated by the $(UO_2)^{2+}$ uranyl ion, a linear molecule with two triply bound oxygen atoms. These strong bonds result in linear hybridization and often limit the growth of the uranyl structures to two dimensions. The dimensionality of uranyl structures can be increased with the addition of organic ligands, transition metals, and/or peroxide to produce frameworks and cage clusters.[2]

The structural hierarchy of inorganic uranyl complexes emphasizes repeating building units that occur across different compounds.[2] Efforts have sought to understand the impact that ligands and counterions have on the coordination chemistry and basic subunits of uranyl compounds.[3,4] Targeted synthesis conditions range from room-temperature self-assembly reactions, as for uranyl peroxide clusters,[5,6] to hydrothermal syntheses,[7] to high-temperature flux-based syntheses.[8] Higher temperatures often promote hydrolysis and the formation of sheet and chain structures. While small molecule organics are known to serve as effective ligands under hydrothermal conditions to generate previously unreported structures, uranyl coordination is difficult to control as hydrolysis and pH offer many variables.[7] An ionothermal synthesis approach involves no water, removing these issues to provide better control of the coordination environments of uranium by reducing the likelihood of hydrolysis reactions.

Ionothermal synthesis consists of the employment of ionic liquids (ILs) as both solvent and structure directing template in the presence of a reactive partner.[9] While ionothermal synthesis often parallels hydrothermal synthesis, in which water is the solvent, the former benefits from leveraging both the cationic and anionic components for the formation of metal−metal or metal−organic frameworks. ILs have emerged as new solvents for synthesizing metal complexes owing to their low vapor pressure and high tunability.[10] Defined as molten salts, ILs exist in a liquid state at temperatures <100 °C, with many liquid at room temperature.[11] The low vapor pressure of ILs makes them superior candidates for large-scale processes, especially when high temperatures (>100 °C) are required.[12] However, the low vapor pressures and often high viscosity of ILs can render traditional crystallization methods (e.g., slow evaporation, liquid diffusion, etc.) problematic. Thus, higher

Received: August 15, 2023
Revised: September 22, 2023
Published: October 10, 2023

https://doi.org/10.1021/acs.cgd.3c00976
Cryst. Growth Des. 2023, 23, 8311−8318

Table 1. Uranium Source and Ionic Liquid Used for Each Reported Structure

structure	uranium source	ionic liquid
[**1**] $(UO_2)(SO_3C_6H_4COO)(NO_3)P(C_4H_9)_4$	40 mg uranyl nitrate	tetrabutylphosphonium 2-sulfobenzoate $[P_{4444}][2\text{-SB}]$
[**2**] $(UO_2)(SO_3C_6H_4COO)(C_2H_3O_2)P(C_4H_9)_4$	40 mg uranyl acetate	$[P_{4444}][2\text{-SB}]$
[**3**] $(UO_2)(SO_3C_6H_4COO)_2(C_6H_{11}N_2)_2(H_2O)$	40 mg uranyl acetate	1-ethyl-3-methylimidizolium 2-sulfobenzoate [emim][2-SB]
[**4**] $(UO_2)_4O_2(SO_3H_{0.5}C_6H_4COO)_4(C_6H_{11}N_2)_2(H_2O)_4$	40 mg uranyl acetate	[emim][2-SB]
[**5**] $(UO_2)_4O_2(SO_3HC_6H_4COO)_4(SO_3HCF_3)_2(H_2O)_9$	30 mg uranyl triflate	[emim][2-SB]
[**6**] $(UO_2)_2(OH)_2(NO_3)_4(C_4H_7N_2)_2$	40 mg uranyl nitrate	tetrabutylphosphonium benzoate $[P_{4444}][PhCO_2]$
[**7**] $(UO_2)_2(C_2O_4)(NO_3)_4(C_6H_{11}N_2)_2$	40 mg uranyl nitrate	[emim][2-SB]
[**8**] $(UO_2)(C_2H_4O_2)(H_2O)$	40 mg uranyl triflate	[emim][Cl]/(ethylene glycol)$_2$
[**9**] $(UO_2)_3OCl(C_2O_4)(C_2HO_3)_2(C_6H_{11}N_2)_2$	40 mg uranyl nitrate	[emim][Cl]/(ethylene glycol)$_2$
[**10**] $(UO_2)_2(C_2O_4)_2(CO_2)(NH_2(CH_3)_2)$	40 mg uranyl nitrate	[emim][Cl]/β-D-glucopyranose

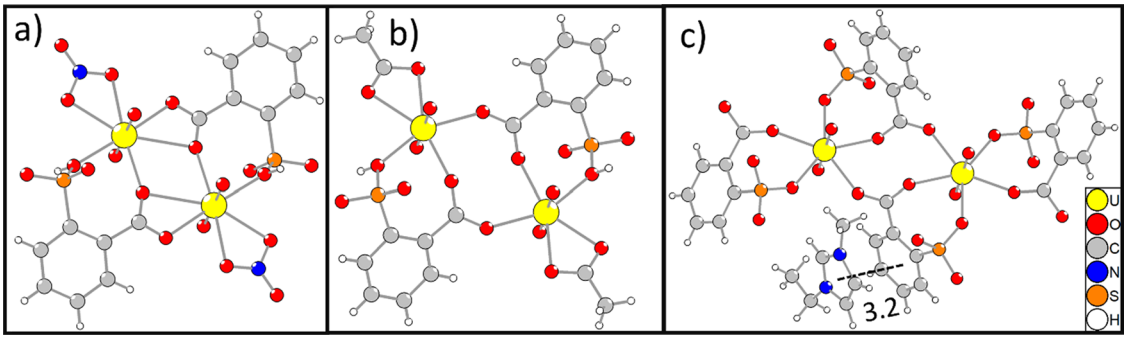

Figure 1. (a) Uranyl dimer in **1**. The stronger coordination of the carboxylate group can be seen as compared to **2**. (b) Uranyl dimer in **2**. Here, the carboxylate is monodentate to each uranyl. (c) Uranyl dimer in **3** with the π-bonding distance between an $[emim]^+$ and the cluster shown. The yellow spheres are uranium, red are oxygen, gray are carbon, blue are nitrogen, orange are sulfur, and white are hydrogen atoms. Some or all of the cations were excluded from each illustration for clarity.

temperatures are used to increase the solubility of reactants in ILs before a slow cooling process promotes crystallization. Furthermore, many ILs are now commercially available, and the vast range of cation−anion combinations allows for the design of task-specific ILs in order to identify those critical structure−function relationships between actinyl crystal growth and IL structure.[11,13,14]

Due to their ready availability, the ILs used to synthesize uranyl compounds are largely imidazolium based. Earlier studies have produced monomeric and dimeric structures built from uranyl ions,[15−21] chains and sheets,[19−29] isolated clusters,[20,30,31] and a few metal−organic frameworks.[24] Existing methods use complex mixtures of ligands or additional metals in combination with the IL and uranium, which renders the predictability of starting material and product solubility challenging.[32] In particular, the addition of solutes to ILs can impact the relative solubilities of other solutes and the properties of the IL itself.[33−35]

Here, we investigated the complexation of the anions of task-specific ILs with uranyl ions to promote crystallization during ionothermal syntheses. The templating role of the IL cation was investigated. Uranium in different starting compounds was used to determine the effect of the salt anion on the final structure and purity of solids. Structures containing formate, glycolate, and oxalate were obtained, and illustrate the propensity for oxidation when nitrate is present. Formulas and crystallographic information for each compound are provided in Table S1.

METHODS

Synthesis. Compounds reported here were synthesized (Table 1) using either uranyl nitrate hexahydrate (International Bio-Analytical Industries, Inc.), uranyl acetate dihydrate (99.3% MV Laboratories, Inc.), or uranyl triflate, which was synthesized according to a reported method.[36] The IL was then added to the uranyl salt with a syringe in a 4 mL Savillex vial. The vials were sealed and placed inside of a 125 mL Teflon lined Parr vessel, placed in an oven at 130 °C for 24 h, and then cooled at 0.1 °C/min to 30 °C. Crystals were stored in the ionic liquid until needed.

While the above are the syntheses from which the reported crystal structures were from, two compounds were synthesized in different solvents. Structure **7** was also observed when uranyl nitrate was added to [emim][Cl]/(glycerin)$_2$. Structure **10** was observed when uranyl nitrate was added to $[P_{4444}]$[*N*-(trifluoroacetyl)leucine], [bmim][bis[(trifluoromethyl) sulfonyl]azanide], [choline][Cl]/(ethylene glycol)$_2$, and [choline][Cl]/β-D-glucopyranose.

The reported compounds were mostly synthesized through differences in the cation of the ionic liquid and the anion of the uranyl salt. The larger $[P_{4444}]$ cation led to the formation of uranyl dimers **1** and **2** that contain nitrate and acetate as well as $[2\text{-SB}]^-$. Using $[emim]^+$ allowed for a tighter packing of the [2-SB] anion in the structures and led to full coordination of uranyl by $[2\text{-SB}]^-$ as in **3** as well as formation of the uranyl tetramer seen in **4** and **5**. Using uranyl triflate led to the isolation of just the tetramer in **5**. Nitrate was found to oxidize many of the ionic liquids during the thermal treatment leading to the glycolate and oxalate seen in some of the reported products.

Single crystal X-ray diffraction data were collected and processed in one of two ways. Some data were collected using a Bruker APEX II Quazar X-ray diffractometer with graphite-monochromated Mo K_α radiation from a microfocus source using an $\omega-\theta$ scanning mode. These data were processed using SAINT[37] and were scaled, merged, and corrected for Lorentz, polarization, and absorption effects using SADABS.[38] Other data were collected using a Rigaku XtaLAB Synergy X-ray diffractometer equipped with a PhotonJet microfocus sealed X-ray tube producing Mo K_α radiation and a HyPix-6000HE detector. These data were processed using CrysAlisPro[39] and were scaled, merged, and corrected for Lorentz, polarization, and

https://doi.org/10.1021/acs.cgd.3c00976
Cryst. Growth Des. 2023, 23, 8311−8318

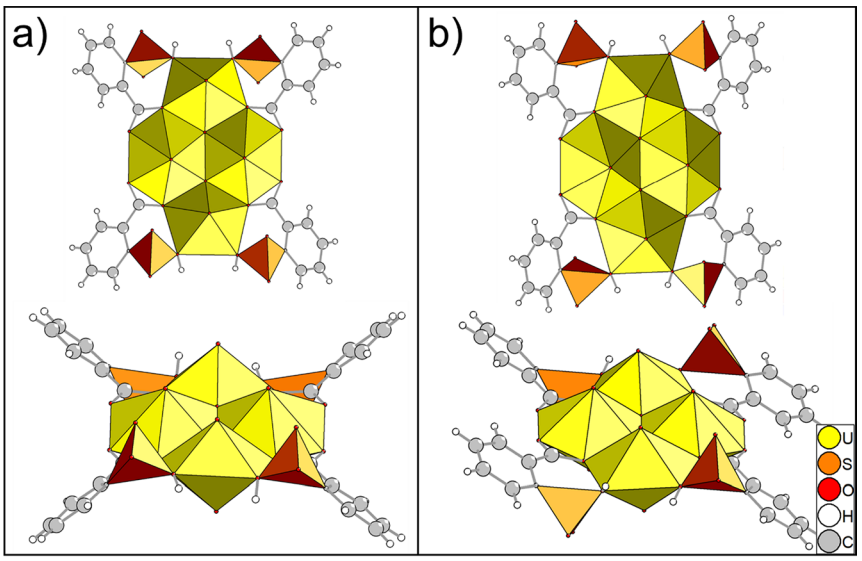

Figure 2. (a) Uranyl tetramer in **4** shown from the top and at an angle. [emim] cations are excluded. The hydrogen sites on the sulfonate groups are all half occupied. (b) Uranyl tetramer in **5** shown from the top and at an angle. Triflic acids are excluded for clarity. The yellow polyhedra are uranium, orange are sulfur, red spheres are oxygen, white are hydrogen, and gray are carbon.

absorption effects using SCALE3 ABSPACK. Data were then imported into either Jana 2006[40] or Olex2 for analysis.

Powder X-ray diffraction data were collected using a Malvern Aeris instrument with a step size of 0.1° and count time of 5 s.

RESULTS AND DISCUSSION

The first system explored used the tetrabutylphosphonium 2-sulfobenzoate $[P_{4444}][2\text{-SB}]$ IL. Using uranyl nitrate afforded crystals of **1** that contains clusters composed of two uranyl ions, each of which is chelated by a nitrate and carboxylate of one $[2\text{-SB}]^-$ as well as monodentate by the carboxylate and sulfonate of the other $[2\text{-SB}]^-$ (Figure 1a). This type of uranyl coordination by the carboxylate and sulfonate of a $[2\text{-SB}]^-$ ligand is hereafter designated as SB-chelation. The cluster in **1** contains two uranium polyhedra coordinated as hexagonal bipyramids that share a polyhedral edge, forming a dimer. Structures with similar dimers of uranyl polyhedra have been published[41−45] although with citrate or 2-hydroxybenzoate-based ligands and were synthesized hydro- or solvothermally. Alongside **1**, multiple uranyl-bearing side products containing oxalate and acetate crystallized in the same vial (these byproducts are discussed in the Supporting Information). It is hypothesized that oxalate and acetate were generated in situ via the oxidative degradation of the alkyl chains present in the $[P_{4444}]$ cation.

To determine if nitrate, from the uranyl nitrate reactant, oxidized the alkyl chains on the $[P_{4444}]$ cation to form oxalate/acetate byproducts, separate reactions were conducted employing uranyl acetate. This resulted in crystals of **2** that exhibit a ligand coordination nearly identical to **1**. The main difference, aside from nitrate being substituted by acetate, is the coordination of $[2\text{-SB}]^-$. Acetate coordinates more strongly to uranyl than nitrate causing the carboxylate group of $[2\text{-SB}]^-$ to only be monodentate to each uranyl ion (Figure 1b) resulting in 7-coordinate instead of 8-coordinate uranium atoms. This placed the uranium atoms in **2** at a separation of 5.51 Å compared to that of 4.37 Å in **1**. Using uranyl acetate resulted in no side products, supporting a mechanism involving nitrate-promoted oxidative degradation of the $[P_{4444}]$ cation.

Potential structure templating effects of the IL cations were investigated by replacing the $[P_{4444}]$ cation with 1-ethyl-3-methylimidazolium $[emim]^+$. This resulted in crystallization of a similar cluster (**3**) as in **1** and **2** except in place of nitrate or acetate there are two additional $[2\text{-SB}]^-$ ligands coordinating to the two uranyl cations (Figure 1c). Exclusion of acetate in **3** occurs because $[emim]^+$ has a charge density higher than that of $[P_{4444}]^+$, allowing for tighter packing of the cation with the anionic cluster. This tighter packing is needed as the two additional 2-SBs give the cluster an additional 2− charge. It is conceivable that a smaller phosphonium cation may aid in the formation of larger clusters or frameworks. However, the size and asymmetry of the cation are key factors in reducing the melting point and viscosity of the IL, presenting future design parameters for task specific ILs to facilitate the purification of actinides.[46]

The anionic cluster in **3** has been described previously with a 4,4′-bipyridinium countercation but was produced under hydrothermal conditions.[47] However, in **3**, disorder of two of the 2-sulfobenzoate ligands occurs because of the SB-chelation to the uranyl ion. This allows the $[2\text{-SB}]^-$ ligand to rotate 180° when bonding to the uranyl ion (Figure S1), and the diffraction data revealed a split 74/26 occupancy of the two sites. This is due to the proximity of one of the $[emim]^+$ cations to the disordered site. Where the sulfonate is on the side closest to the $[emim]^+$, there are H···A distances of 3.09 Å between H8 and O14, and 1.74 Å between H28 and O14. This latter distance is short for hydrogen bonds of the C−H···O type and causes strain on the structure.[48,49] This can be seen not only via the disorder of the $[2\text{-SB}]^-$ but also in the displacement parameters of the nearby $[emim]^+$. The displacement ellipsoids are considerably larger than those of the other $[emim]^+$ in the structure (Figure S2) as the cation must shift to accommodate the additional oxygen of the sulfonate. When the sulfonate is in the more occupied site, the C−H···O distances are more common at 2.52 Å between H8 and O13, and 2.63 Å between H28 and O13 thus making it the favored position.

Compounds **1**−**3** show no evidence of hydrolysis. However, the coordinated water in the uranium source could promote

https://doi.org/10.1021/acs.cgd.3c00976
Cryst. Growth Des. 2023, 23, 8311−8318

hydrolysis in the reaction that produced **4**, which is a tetramer of uranyl ions capped by four $[2\text{-SB}]^-$ ligands (Figure 2a). The tetramer of uranyl ions in **4** contains two μ_3−O bridges connecting two hexagonal and two pentagonal bipyramids. The uranyl ions of the hexagonal bipyramids are chelated by the carboxylate of the $[2\text{-SB}]^-$ ligands whereas the uranyl ions of the pentagonal bipyramids are SB-chelated (Figure 2a). The cluster is charge balanced by two [emim] cations with the space between occupied by water. There are no π interactions between the $[2\text{-SB}]^-$ and $[\text{emim}]^+$ rings. Instead, the [emim] cations hydrogen bond to the uranyl ions and sulfonate groups of the clusters. The anionic cluster has been reported before[50] with 2-carboxybenzoate,[51−54] but, again, were synthesized hydrothermally.

The products that provided crystals of **3** and **4**, whose structures lack acetate or nitrate contained significant amounts of side products that incorporate nitrate, acetate, or oxalate. To probe the strength of ligand coordination of the uranium stock on the reaction outcome, additional reactions were conducted using uranyl Triflate ($UO_2SO_3CF_3$, UOTf). triflate does not coordinate uranyl as strongly as nitrate or acetate due to inductive effects. This produced **5** that contains an isomeric cluster similar to that seen in **4**. The key difference is in the protonation and conformation of the ligands on the cluster. The sulfonates on **4** are only half protonated (i.e., only two are protonated locally), whereas in the structure of **5**, all four are protonated, resulting in an electroneutral cluster. The different protonation states impact how the ligands coordinate to the cluster and how the clusters pack into the extended structure. In the case of **4**, the phenyl rings of the 2-SBs on the short side of the cluster are oriented in the same direction, either above or below the cluster (Figure 2a). However, the phenyl rings of the ligands on the long side of the cluster in **5** are oriented in the same direction (Figure 2b). The clusters in **5** are π-bonded to each other through two of the 2-SB ligands with a centroid-to-centroid distance of 3.76 Å (Figure 3a). The rings define infinite planes that are almost parallel (they are inclined to each other by 3°). These two rings form "tubes" through weaker π-stacking with 2-SBs of other clusters (Figure 3b). The structure contains triflic acid surrounded by water molecules that in turn are H-bonded to the tetramers. The conformation and high protonation of the tetramer in **5** has not been previously reported. Instead, all published structures of this uranium tetramer with benzoate ligands take on the conformation of **4**.

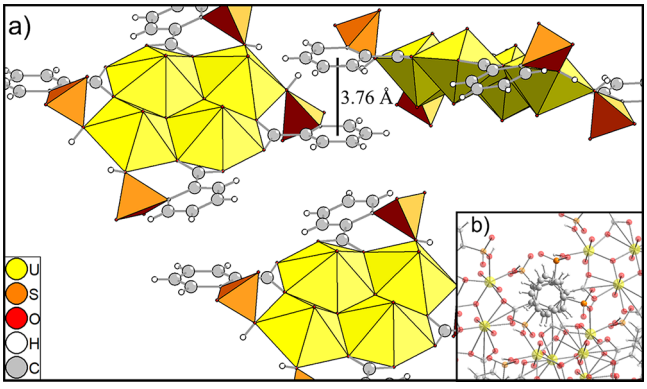

Figure 3. (a) Uranyl tetramers of **5** showing the π-bonding between the benzene rings of the 2-SB ligands. The ligands with opposite corners participate in one strong π−π interaction and one weak π−π interaction. The other two ligands participate in two weak π−π interactions. (b) Benzene rings of the ligands arrange in one dimension to form "tubes" which can be looked down as shown here. The yellow polyhedra are uranium, orange are sulfur, red spheres are oxygen, white are hydrogen, and gray are carbon.

The various side products obtained in the previously reported reactions presented interesting structures and provided insights into the mechanistic pathways accessed when utilizing task-specific ILs. Many of these products contained fragments of IL, most of which had been oxidized. When $[\text{emim}]^+$ is broken down, the ethyl group is oxidatively cleaved as in **6**, which contains an isolated methyl imidazole cation (Figure 4a).[55] The detached ethyl group from $[\text{emim}]^+$ oxidizes to form an oxalate ion that can bridge uranyl ions, such as in **7** (Figure 4b). However, oxalate could also be contributed from $[P_{4444}]^+$ as its ^{n}butyl chains are susceptible to oxidation by nitrate at elevated temperatures. The oxalate ion strongly bonds to uranyl to form a variety of structures ranging from truncated clusters to extended sheets. Compound **7** contains a dimer of uranyl ions bridged by an oxalate and capped by four nitrate groups. This dimer has been reported with multiple organic counter cations, and in all cases, the oxalate was generated from oxidation of an organic as in our structure.[56−59] Many of the syntheses also contained crystals of uroxite, a uranyl oxalate mineral made up of extended sheets,[60] or a uranyl oxalate hydrate chain reported by Giesting et al.[61] When complexation by the anion of the IL did not occur, there were often crystals of [emim] uranyl triacetate/trinitrate[62,63] or the dimer in **6** (Figure 4a) with [emim] as the cation.[64] The exact conditions leading to the formation of these side products are reported in the Supporting Information.

Considering oxalate was the most prevalent product of imidazolium oxidative cleavage observed, we determined the effect of time on oxidation as well as the complexation of less oxidized two-carbon chains to uranyl. To that end, [emim][Cl] and ethylene glycol (2 equiv) were used in conjunction with uranyl triflate and afforded crystals of **8**, containing the uranyl ethylene glycol water chain (Figure 4c). Ethylene glycol is fully deprotonated, forming a bidentate chelation with one uranyl while serving as a bridge to the second and third uranyl ion in the chain.

If uranyl nitrate is used in place of uranyl triflate, oxidation produces oxalate and the intermediate glycolate. Structure **9** is a uranyl oxalate glycolate sheet consisting of uranyl trimers, each with a central μ_3-O, which are bridged by one oxalate and four glycolate groups and capped with a chloride (Figure 5a). Pairs of trimers are bridged by oxalate that causes them to lie parallel to each other. These pairs alternate directions, causing corrugation, via the glycolate ligands that do not form such rigid planar bridges with uranyl as we observed with oxalate. The sheets are separated, and charge balanced, by [emim] cations that H-bond to the oxygen atoms of the uranyl cations and one oxygen of a glycolate (Figure 5b). A ball and stick model of the uranyl trimer and its coordinating ligands are shown in Figure 5c.

Compound **10** was crystallized with the deep eutectic solvent [choline][Cl]/β-D-glucopyranose. The structure in **10** consists of a uranyl oxalate chain bridged by formate to form sheets that yield a hexameric ring charge balanced by dimethylammonium cations (Figure 6). These cations, as well as oxalate and formate, arise from the degradation and oxidation of [choline]. The cations are located next to an inversion center and are disordered, facing both above and

https://doi.org/10.1021/acs.cgd.3c00976
Cryst. Growth Des. 2023, 23, 8311−8318

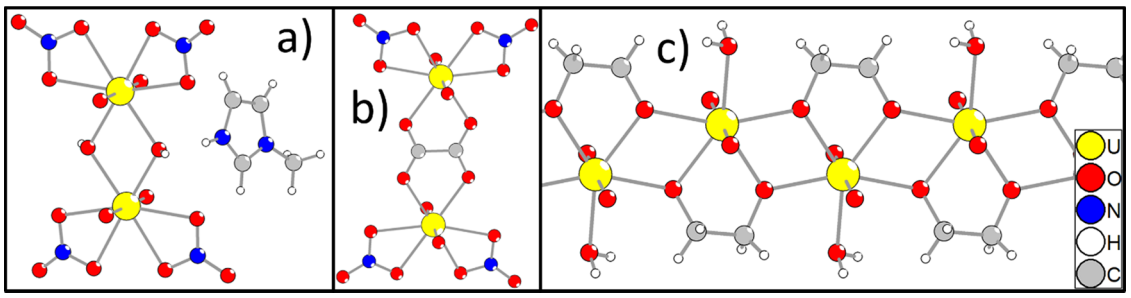

Figure 4. (a) Structure **6** that contains methyl imidazolium. (b) Structure **7**, which is similar to the cluster of **6** but with an oxalate bridging the uranyl ions instead of two hydroxides. [emim] cations were removed. (c) Structure **8** which is composed of uranyl cations connected by 1,2-ethanediol and capped with water. The yellow spheres are uranium, red are oxygen, blue are nitrogen, white are hydrogen, and gray are carbon atoms.

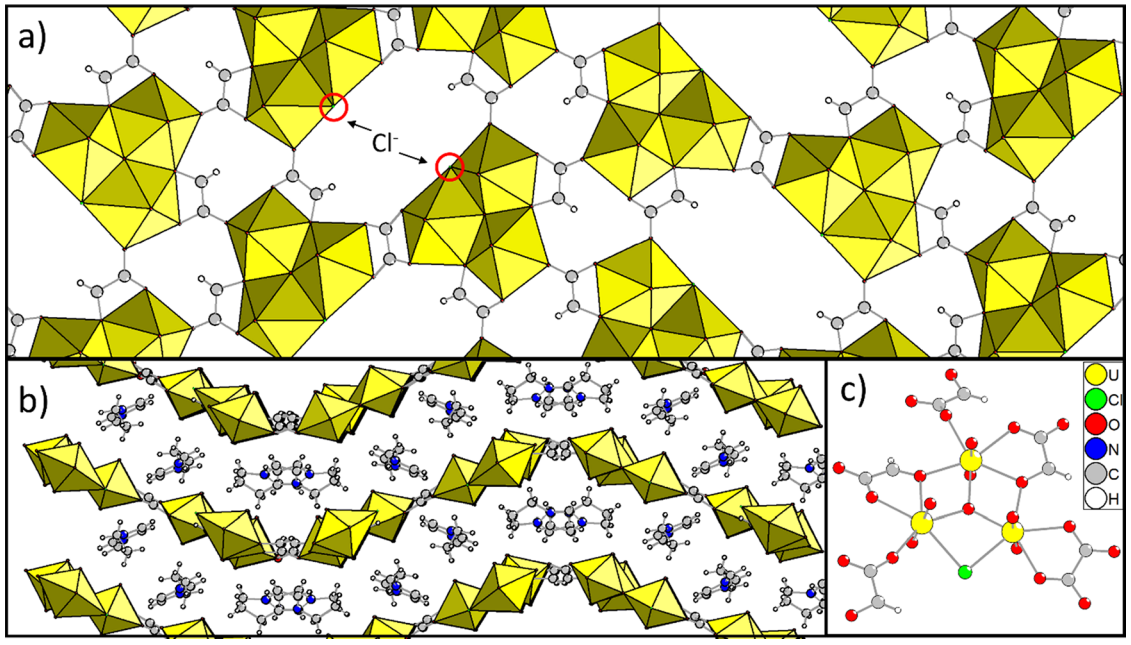

Figure 5. (a) Top-down view of the sheet in **9**. Two of the chloride anions are circled in red. [emim] cations are omitted for clarity. (b) Stacking of the sheets and interlayers of **9** as viewed down the *c*-axis with [emim] cations filling the interlayers. (c) Ball and stick representation of the trimer in **9** showing the coordination of ligands. The yellow spheres are uranium, green are chloride, red are oxygen, blue are nitrogen, gray are carbon, and white are hydrogen atoms.

below the sheets. The formate ion is also disordered as the carbon atom can face either toward or away from the dimethylammonium. This structure is similar to that of alkali metal uranyl oxalate hydrates synthesized by Giesting et al.,[61] which contains a hydroxide bridge instead of a formate bridge.

Subsequent to parameter optimization of the ionothermal syntheses for pure product formation, a uranyl succinate framework was chosen to test the viability of this method.[65] The framework is electroneutral with a 1:1 uranyl:succinate ratio that is optimal for precipitation from the IL. Ionothermal treatment of uranyl Triflate in [P_{4444}][succinate] produce elongated diamond-shaped crystals that have the same unit cell as the reported synthesis[65] and powder X-ray diffraction showed it to be pure aside from a small succinic acid impurity (Figure S3). Curiously, uranium failed to precipitate from [emim][succinate] after ionothermal treatment. When additional uranyl triflate was added after the second ionothermal cycle, the resulting ternary IL solidified. This suggests that larger bulker cations would be better suited for framework syntheses using this method as the resulting products would likely form a room-temperature ionic liquid.

CONCLUSIONS

This work presents an alternative preparation of actinide clusters, whereby ILs are capable of serving as both solvents and ligands in a bifunctional fashion during ionothermal assembly. The aforementioned methodology simplifies the reaction protocol by minimizing the number of oxidizing agents and superfluous reagents and promotes isolation via crystallization directly from the reaction media. Examination of various uranyl salts revealed that uranyl triflate proved to be an optimal source of actinide in the formation of metal clusters/sheets in high purity. In contrast, employing uranyl nitrate led to oxidation of the parent IL to generate glycolate and oxalate byproducts, along with new and unusual structures such as **9**. Many of the ILs used were designed specifically to incorporate anions known to coordinate with uranyl centers. Additionally, the developed ionothermal synthesis avoids the need for modulators, which are often used in metal−organic framework

https://doi.org/10.1021/acs.cgd.3c00976
Cryst. Growth Des. 2023, 23, 8311−8318

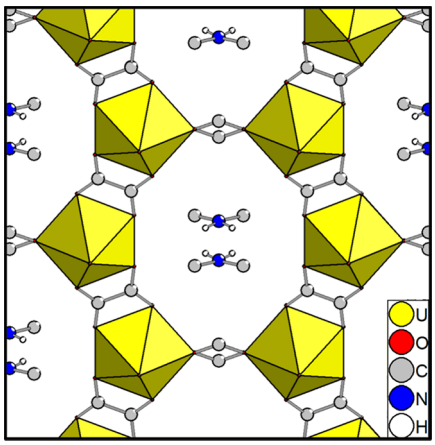

Figure 6. Sheets in **10**, as viewed down the *c*-axis, are composed of repeating hexameric "rings" of uranyl, oxalate, and formate. The disorder of the formate and dimethylammonium is shown. The yellow polyhedra are uranium, red are oxygen, gray are carbon, blue are nitrogen, and white are hydrogen atoms.

syntheses. Future efforts will focus on the synthesis and implementation of designer ILs containing alternative anionic components for the production of uranyl clusters and determining the role of the cation to identify the stereo-electronic factors that contribute to the formation of these unusual extended frameworks.

■ ASSOCIATED CONTENT

Supporting Information

The Supporting Information is available free of charge at https://pubs.acs.org/doi/10.1021/acs.cgd.3c00976.

Fragment of the cluster in **3** showing the disorder of the 2-sulfobenzoate ligand; disordered 2-sulfobenzoate of **3** and the proximity of the nearby 1-ethyl-3-methylimadazolium ([emim]) cations; experimental and calculated PXRD patterns of the uranyl succinate framework synthesized from uranyl triflate and [P4444][succinate]; and crystallographic information and refinements parameters for reported structures (PDF)

Accession Codes

CCDC 2287827−2287836 contain the supplementary crystallographic data for this paper. These data can be obtained free of charge via www.ccdc.cam.ac.uk/data_request/cif, or by emailing data_request@ccdc.cam.ac.uk, or by contacting The Cambridge Crystallographic Data Centre, 12 Union Road, Cambridge CB2 1EZ, U.K.; fax: +44 1223 336033.

■ AUTHOR INFORMATION

Corresponding Authors

Brandon L. Ashfeld − *Department of Chemistry and Biochemistry, University of Notre Dame, Notre Dame, Indiana 46556, United States;* orcid.org/0000-0002-4552-2705; Email: bashfeld@nd.edu

Peter C. Burns − *Department of Chemistry and Biochemistry, University of Notre Dame, Notre Dame, Indiana 46556, United States; Department of Civil and Environmental Engineering and Earth Sciences, University of Notre Dame, Notre Dame, Indiana 46556, United States;* orcid.org/0000-0002-2319-9628; Email: pburns@nd.edu

Authors

Daniel E. Felton − *Department of Chemistry and Biochemistry, University of Notre Dame, Notre Dame, Indiana 46556, United States*

Tsuyoshi A. Kohlgruber − *Department of Civil and Environmental Engineering and Earth Sciences, University of Notre Dame, Notre Dame, Indiana 46556, United States; Pacific Northwest National Laboratory, Richland, Washington 99354, United States*

Zachary D. Tucker − *Department of Chemistry and Biochemistry, University of Notre Dame, Notre Dame, Indiana 46556, United States*

Eva M. Gulotty − *Department of Chemistry and Biochemistry, University of Notre Dame, Notre Dame, Indiana 46556, United States*

Complete contact information is available at: https://pubs.acs.org/10.1021/acs.cgd.3c00976

Author Contributions

The manuscript was written through contributions of all authors. All authors have given approval to the final version of the manuscript.

Funding

The work in this manuscript was supported in part by the National Science Foundation CHE-1956170 and CBET-2031431 (B.L.A.).

Notes

The authors declare no competing financial interest.

■ REFERENCES

(1) Groom, C. R.; Bruno, I. J.; Lightfoot, M. P.; Ward, S. C. The Cambridge Structural Database. *Acta Crystallogr. Sect. B Struct. Sci. Cryst. Eng. Mater.* **2016**, *72* (Pt 2), 171−179.

(2) Lussier, A. J.; Lopez, R. A. K.; Burns, P. C. A Revised and Expanded Structure Hierarchy of Natural and Synthetic Hexavalent Uranium Compounds. *Can. Mineral.* **2016**, *54* (1), 177−283.

(3) An, S.; Mei, L.; Hu, K.; Li, F.; Xia, C.; Chai, Z.; Shi, W. Bipyridine-Directed Syntheses of Uranyl Compounds Containing Semirigid Dicarboxylate Linkers: Diversity and Consistency in Uranyl Speciation. *Inorg. Chem.* **2019**, *58* (10), 6934−6945.

(4) Misra, A.; Kozma, K.; Streb, C.; Nyman, M. Beyond Charge Balance: Counter-Cations in Polyoxometalate Chemistry. *Angew. Chem., Int. Ed.* **2020**, *59* (2), 596−612.

(5) Burns, P. C.; Nyman, M. Captivation with Encapsulation: A Dozen Years of Exploring Uranyl Peroxide Capsules. *Dalton Trans.* **2018**, *47* (17), 5916−5927.

(6) Yang, G.-P.; Li, K.; Hu, C.-W. Recent Advances in Uranium-Containing Polyoxometalates. *Inorg. Chem. Front.* **2022**, *9* (21), 5408−5433.

(7) Andrews, M. B.; Cahill, C. L. Uranyl Bearing Hybrid Materials: Synthesis, Speciation, and Solid-State Structures. *Chem. Rev.* **2013**, *113* (2), 1121−1136.

(8) A. Juillerat, C.; V. Klepov, V.; Morrison, G.; A. Pace, K.; Loye, H.-C. zur Flux Crystal Growth: A Versatile Technique to Reveal the Crystal Chemistry of Complex Uranium Oxides. *Dalton Trans.* **2019**, *48* (10), 3162−3181.

(9) Morris, R. E. Ionothermal Synthesis—Ionic Liquids as Functional Solvents in the Preparation of Crystalline Materials. *Chem. Commun.* **2009**, *21*, 2990.

(10) Zhang, T.; Doert, T.; Wang, H.; Zhang, S.; Ruck, M. Inorganic Synthesis Based on Reactions of Ionic Liquids and Deep Eutectic Solvents. *Angew. Chem., Int. Ed.* **2021**, *60* (41), 22148−22165.

(11) Rogers, R. D.; Seddon, K. R. Ionic Liquids–Solvents of the Future? *Science* **2003**, *302* (5646), 792−793.

(12) V. Plechkova, N.; R. Seddon, K. Applications of Ionic Liquids in the Chemical Industry. *Chem. Soc. Rev.* **2008**, *37* (1), 123−150.
(13) Sanadhya, S.; Tucker, Z. D.; Gulotty, E. M.; Boggess, W.; Ashfeld, B. L.; Moghaddam, S. Thermodynamic Descriptors of Sensible Heat Driven Liquid-Liquid Phase Separation. *J. Mol. Liq.* **2022**, *360*, No. 119440.
(14) Guo, J.; Tucker, Z. D.; Wang, Y.; Ashfeld, B. L.; Luo, T. Ionic Liquid Enables Highly Efficient Low Temperature Desalination by Directional Solvent Extraction. *Nat. Commun.* **2021**, *12* (1), 437.
(15) Lermontov, A. S.; Lermontova, E. Kh.; Wang, Y.-Y. Synthesis, Structure and Optic Properties of 2-Methylimidazolium and 2-Phenylimidazolium Uranyl Acetates. *Inorg. Chim. Acta* **2009**, *362* (10), 3751−3755.
(16) Chen, X.-Y.; Goff, G. S.; Quiroz-Guzman, M.; Fagnant, D. P.; Brennecke, J. F.; Scott, B. L.; Runde, W. Directed Nucleation of Monomeric and Dimeric Uranium(vi) Complexes with a Room Temperature Carboxyl-Functionalized Phosphonium Ionic Liquid. *Chem. Commun.* **2013**, *49* (19), 1903.
(17) Qu, F.; Zhu, Q.-Q.; Liu, C.-L. Crystallization in Ionic Liquids: Synthesis, Properties, and Polymorphs of Uranyl Salts. *Cryst. Growth Des.* **2014**, *14* (12), 6421−6432.
(18) Yaprak, D.; Spielberg, E. T.; Bäcker, T.; Richter, M.; Mallick, B.; Klein, A.; Mudring, A.-V. A Roadmap to Uranium Ionic Liquids: Anti-Crystal Engineering. *Chem. - Eur. J.* **2014**, *20* (21), 6482−6493.
(19) Smith, P. A.; Burns, P. C. Ionothermal Effects on Low-Dimensionality Uranyl Compounds Using Task Specific Ionic Liquids. *CrystEngComm* **2014**, *16* (31), 7244−7250.
(20) Parker, T. G.; Cross, J. N.; Polinski, M. J.; Lin, J.; Albrecht-Schmitt, T. E. Ionothermal and Hydrothermal Flux Syntheses of Five New Uranyl Phosphonates. *Cryst. Growth Des.* **2014**, *14* (1), 228−235.
(21) Nockemann, P.; Van Deun, R.; Thijs, B.; Huys, D.; Vanecht, E.; Van Hecke, K.; Van Meervelt, L.; Binnemans, K. Uranyl Complexes of Carboxyl-Functionalized Ionic Liquids. *Inorg. Chem.* **2010**, *49* (7), 3351−3360.
(22) Wylie, E. M.; Dustin, M. K.; Smith, J. S.; Burns, P. C. Ionothermal Synthesis of Uranyl Compounds That Incorporate Imidazole Derivatives. *J. Solid State Chem.* **2013**, *197*, 266−272.
(23) Zheng, T.; Gao, Y.; Chen, L.; Diwu, J.; Chai, Z.; Albrecht-Schmitt, T. E.; Wang, S. Structural and Spectroscopic Characterization of Two New Layered Uranyl(VI) p-Xylenediphosphonate Compounds Synthesized via Ionothermal Method. *Inorg. Chim. Acta* **2015**, *435*, 131−136.
(24) Zheng, T.; Gao, Y.; Chen, L.; Liu, Z.; Diwu, J.; Chai, Z.; Albrecht-Schmitt, T. E.; Wang, S. A New Chiral Uranyl Phosphonate Framework Consisting of Achiral Building Units Generated from Ionothermal Reaction: Structure and Spectroscopy Characterizations. *Dalton Trans.* **2015**, *44* (41), 18158−18166.
(25) Smith, P. A.; Aksenov, S. M.; Jablonski, S.; Burns, P. C. Structural Unit Charge Density and Molecular Cation Templating Effects on Orientational Geometric Isomerism and Interlayer Spacing in 2-D Uranyl Sulfates. *J. Solid State Chem.* **2018**, *266*, 286−296.
(26) Wang, F.; Mei, L.; Shi, W.; Chu, T. Synthesis and Crystal Structures of Two New Uranyl Coordination Compounds Obtained in Aqueous Solutions of 1-Butyl-2,3-Dimethylimidazolium Chloride. *J. Coord. Chem.* **2018**, *71* (15), 2415−2425.
(27) Kohlgruber, T. A.; Mackley, S. A.; Bo, F. D.; Aksenov, S. M.; Burns, P. C. The Role of 1-Ethyl-3-Methylimidazolium Diethyl Phosphate Ionic Liquid in Uranyl Phosphate Compounds. *J. Solid State Chem.* **2019**, *279*, No. 120938.
(28) Kohlgruber, T. A.; Felton, D. E.; Perry, S. N.; Oliver, A. G.; Burns, P. C. Effect of Ionothermal Conditions on the Crystallization of Organically Templated Uranyl Sulfate Compounds. *Cryst. Growth Des.* **2021**, *21* (2), 861−868.
(29) Kohlgruber, T. A.; Perry, S. N.; Sigmon, G. E.; Oliver, A. G.; Burns, P. C. Hydrogen Bond Network and Bond Valence Analysis on Uranyl Sulfate Compounds with Organic-Based Interstitial Cations. *J. Solid State Chem.* **2022**, *307*, No. 122871.
(30) Senchyk, G. A.; Wylie, E. M.; Prizio, S.; Szymanowski, J. E. S.; Sigmon, G. E.; Burns, P. C. Hybrid Uranyl−Vanadium Nano-Wheels. *Chem. Commun.* **2015**, *51* (50), 10134−10137.
(31) Kohlgruber, T. A.; Senchyk, G. A.; Rodriguez, V. G.; Mackley, S. A.; Dal Bo, F.; Aksenov, S. M.; Szymanowski, J. E. S.; Sigmon, G. E.; Oliver, A. G.; Burns, P. C. Ionothermal Synthesis of Uranyl Vanadate Nanoshell Heteropolyoxometalates. *Inorg. Chem.* **2021**, *60*, 3355.
(32) Karmakar, A.; Mukundan, R.; Yang, P.; Batista, R.; E. Solubility Model of Metal Complex in Ionic Liquids from First Principle Calculations. *RSC Adv.* **2019**, *9* (32), 18506−18526.
(33) Shinkle, A. A.; Pomaville, T. J.; Sleightholme, A. E. S.; Thompson, L. T.; Monroe, C. W. Solvents and Supporting Electrolytes for Vanadium Acetylacetonate Flow Batteries. *J. Power Sources* **2014**, *248*, 1299−1305.
(34) Gulotty, E. M.; Sanadhya, S.; Tucker, Z. D.; Moghaddam, S. S.; Ashfeld, B. L. Controlling Phase Separation Behavior of Thermo-Responsive Ionic Liquids through the Directed Distribution of Anionic Charge. *J. Mol. Liq.* **2022**, *360*, No. 119401.
(35) Bhagwat, R.; Sanadhya, S.; Gulotty, E.; Tucker, Z.; Ashfeld, B.; Moghaddam, S. High-Precision Vapor Pressure Measurement Apparatus with Facile and Inexpensive Construction. *Meas. Sci. Technol.* **2022**, *33* (6), No. 067002.
(36) Berthet, J. C.; Lance, M.; Nierlich, M.; Ephritikhine, M. Simple Preparations of the Anhydrous and Solvent-Free Uranyl and Cerium(IV) Triflates $UO_2(OTf)_2$ and $Ce(OTf)_4$ − Crystal Structures of $UO_2(OTf)_2(Py)_3$ and $[\{UO_2(Py)_4\}_2(\mu\text{-}O)][OTf]_2$. *Eur. J. Inorg. Chem.* **2000**, *2000* (9), 1969−1973.
(37) *SAINT*; Bruker AXS Inc.: Wisconsin (USA), Madison, 2012.
(38) *SADABS*; Bruker AXS Inc.: Wisconsin (USA), Madison, 2001.
(39) *CrysAlis^{Pro}* version 1.171.40.58a; Rigaku Corporation: Wroclaw (Poland), 2019.
(40) Petříček, V.; Dušek, M.; Palatinus, L. Crystallographic Computing System JANA2006: General Features. *Z. Krist. - Cryst. Mater.* **2014**, *229* (5), 1737.
(41) Bharara, M. S.; Strawbridge, K.; Vilsek, J. Z.; Bray, T. H.; Gorden, A. E. V. Novel Dinuclear Uranyl Complexes with Asymmetric Schiff Base Ligands: Synthesis, Structural Characterization, Reactivity, and Extraction Studies. *Inorg. Chem.* **2007**, *46* (20), 8309−8315.
(42) Basile, M.; Unruh, D. K.; Flores, E.; Johns, A.; Forbes, T. Z. Structural Characterization of Environmentally Relevant Ternary Uranyl Citrate Complexes Present in Aqueous Solutions and Solid State Materials. *Dalton Trans.* **2015**, *44* (6), 2597−2605.
(43) Nassimbeni, L. R.; Rodgers, A. L.; Haigh, J. M. The Crystal and Molecular Structure of the Bis(4-N,N′-Dimethylaminopyridine) Solvate of Di-μ-Salicylicacidato Bis{nitratodioxouranium(VI)}. *Inorg. Chim. Acta* **1976**, *20*, 149−153.
(44) Singh, J.; Yadav, D.; Singh, J. D. En Route Activity of Hydration Water Allied with Uranyl (UO_2^{2+}) Salts Amid Complexation Reactions with an Organothio-Based (O, N, S) Donor Base. *Inorg. Chem.* **2019**, *58* (8), 4972−4978.
(45) Thuéry, P. Solvothermal Synthesis and Crystal Structure of Uranyl Complexes with 1,1-Cyclobutanedicarboxylic and (1R,3S)-(+)-Camphoric Acids − Novel Chiral Uranyl-Organic Frameworks. *Eur. J. Inorg. Chem.* **2006**, *2006* (18), 3646−3651.
(46) Endo, T.; Sunada, K.; Sumida, H.; Kimura, Y. Origin of Low Melting Point of Ionic Liquids: Dominant Role of Entropy. *Chem. Sci.* **2022**, *13* (25), 7560−7565.
(47) Thuéry, P. Sulfonate Complexes of Actinide Ions: Structural Diversity in Uranyl Complexes with 2-Sulfobenzoate. *Inorg. Chem.* **2013**, *52* (1), 435−447.
(48) Severa, G.; Bruffey, E.; Nguyen, P. Q. H.; Gigante, A.; Leick, N.; Kelly, C.; Finkelstein, G. J.; Hagemann, H.; Gennett, T.; Rocheleau, R. E.; Dera, P. $Fe_4(OAc)_{10}[EMIM]_2$: Novel Iron-Based Acetate EMIM Ionic Compound. *ACS Omega* **2021**, *6* (47), 31907−31918.
(49) Itoh, Y.; Nakashima, Y.; Tsukamoto, S.; Kurohara, T.; Suzuki, M.; Sakae, Y.; Oda, M.; Okamoto, Y.; Suzuki, T. N+-C-H···O

https://doi.org/10.1021/acs.cgd.3c00976
Cryst. Growth Des. 2023, 23, 8311−8318

Hydrogen Bonds in Protein-Ligand Complexes. *Sci. Rep.* **2019**, *9* (1), 767.
(50) Thuéry, P. Molecular and Polymeric Uranyl and Thorium Complexes with Sulfonate-Containing Ligands. *Eur. J. Inorg. Chem.* **2014**, *2014* (1), 58−68.
(51) Andreev, G.; Budantseva, N.; Levtsova, A.; Sokolova, M.; Fedoseev, A. Formation of Uranyl Phthalate Coordination Polymers with Unusual 2D Net Topologies in the Presence of Organic Cations. *CrystEngComm* **2020**, *22* (48), 8394−8404.
(52) Charushnikova, I. A.; Krot, N. N.; Polyakova, I. N.; Makarenkov, V. I. Synthesis of Double Uranyl Phthalates of the $M_4[(UO_2)_4(\mu_3\text{-}O)_2(C_6H_4C_2O_4)_4] \cdot nH_2O$ Type with M = NH_4, K, and Cs. Crystal Structure of $K_4[(UO_2)_4O_2(C_6H_4C_2O_4)_4] \cdot 3H_2O$. *Radiochemistry* **2005**, *47* (3), 241−246.
(53) Thuéry, P.; Harrowfield, J. $[Ni(Cyclam)]^{2+}$ and $[Ni(R,S\text{-}Me_6Cyclam)]^{2+}$ as Linkers or counterions In Uranyl−Organic Species with Cis- and Trans-1,2-Cyclohexanedicarboxylate Ligands. *Cryst. Growth Des.* **2018**, *18* (9), 5512−5520.
(54) Thuéry, P.; Harrowfield, J. Contrasting Structure-Directing Effects in the Uranyl−Phthalate/Isophthalate Isomer Systems. *Cryst. Growth Des.* **2021**, *21* (5), 3000−3013.
(55) Shiryaev, A. A.; Fedoseev, A. M.; Grigor'ev, M. S.; Averin, A. A. Synthesis, Structure, and Spectral Properties of Mixed Uranyl Hydroxonitrate Complexes $[(CH_3)_4N]_2[(UO_2)_2(NO_3)_4(OH)_2]$ and $(HMeIm)_2[(UO_2)_2(NO_3)_4(OH)_2]$ (MeIm = 1-Methylimidazole). *Radiochemistry* **2018**, *60* (5), 507−513.
(56) Bradley, A. E.; Hardacre, C.; Nieuwenhuyzen, M.; Pitner, W. R.; Sanders, D.; Seddon, K. R.; Thied, R. C. A Structural and Electrochemical Investigation of 1-Alkyl-3-Methylimidazolium Salts of the Nitratodioxouranate(VI) Anions $[\{UO_2(NO_3)_2\}_2(M4\text{-}C_2O_4)]^{2-}$, $[UO_2(NO_3)_3]^-$, and $[UO_2(NO_3)_4]^{2-}$. *Inorg. Chem.* **2004**, *43* (8), 2503−2514.
(57) Bradley, A. E.; Hatter, J. E.; Nieuwenhuyzen, M.; Pitner, W. R.; Seddon, K. R.; Thied, R. C. Precipitation of a Dioxouranium(VI) Species from a Room Temperature Ionic Liquid Medium. *Inorg. Chem.* **2002**, *41* (7), 1692−1694.
(58) Rogers, R. D.; Bond, A. H.; Hipple, W. G.; Rollins, A. N.; Henry, R. F. Synthesis and Structural Elucidation of Novel Uranyl-Crown Ether Compounds Isolated from Nitric, Hydrochloric, Sulfuric, and Acetic Acids. *Inorg. Chem.* **1991**, *30* (12), 2671−2679.
(59) Belomestnykh, V. I.; Sveshnikova, L. B.; Mikhailov, Yu. N. Synthesis and Structure of the Oxalatotetranitratouranylate Complex $(NH_4)_2[\{UO_2(NO_3)_2\}_2(M4\text{-}C_2O_4)] \cdot 2H_2O$. *Russ. J. Inorg. Chem.* **2013**, *58* (6), 664−670.
(60) Kampf, A. R.; Plášil, J.; Nash, B. P.; Němec, I.; Marty, J. uroxite and Metauroxite, the First Two Uranyl Oxalate Minerals. *Mineral. Mag.* **2020**, *84* (1), 131−141.
(61) Giesting, P. A.; Porter, N. J.; Burns, P. C. Uranyl Oxalate Hydrates: Structures and IR Spectra. *Z. Krist. - Cryst. Mater.* **2006**, *221* (4), 252−259.
(62) Kelley, S. P.; Smetana, V.; Emerson, S. D.; Mudring, A.-V.; Rogers, R. D. Benchtop Access to Anhydrous Actinide N-Donor Coordination Complexes Using Ionic Liquids. *Chem. Commun.* **2020**, *56* (30), 4232−4235.
(63) Smetana, V.; Kelley, S. P.; Titi, H. M.; Hou, X.; Tang, S.-F.; Mudring, A.-V.; Rogers, R. D. Synthesis of Anhydrous Acetates for the Components of Nuclear Fuel Recycling in Dialkylimidazolium Acetate Ionic Liquids. *Inorg. Chem.* **2020**, *59* (1), 818−828.
(64) Cocalia, V.; Smiglak, M.; Kelley, S. P.; Shamshina, J. L.; Gurau, G.; Rogers, R. D. Crystallization of Uranyl Salts from Dialkylimidazolium Ionic Liquids or Their Precursors. *Eur. J. Inorg. Chem.* **2010**, *2010* (18), 2760−2767.
(65) Bombieri, G.; Benetollo, F.; Del Pra, A.; Rojas, R. Structural Studies on the Actinide Carboxylates—IV The Crystal and Molecular Structure of Succinate Dioxouranium(VI) Monohydrate. *J. Inorg. Nucl. Chem.* **1979**, *41* (2), 201−203.

https://doi.org/10.1021/acs.cgd.3c00976
Cryst. Growth Des. 2023, 23, 8311−8318